Astrochemical Constraints on the Cosmic-Ray Ionization Rate

Nick Indriolo

1.   INTRODUCTION

Cosmic rays play an extremely important role in the chemistry of the interstellar medium (ISM) by acting as the primary ionization source in regions where the density severely limits the entry of high energy photons. The ions produced by cosmic rays then drive the chemistry in such environments via various ion-molecule reactions. The ionization of H creates free protons which can lead to the production of molecules such as OH and HD. Some polyatomic ions, such as H_3^+ and HCO^+, are formed starting from reactions between the ambient gas and ionized molecular hydrogen, H_2^+. The ion-molecule reactions that form these simple molecules are also responsible for the creation of many of the more complex molecules detected in the ISM.

While the ionization rate is an important parameter in any astrochemical model, its value is only known to within about an order of magnitude. There are a few main reasons for this uncertainty. The low energy ($\lesssim 100$ MeV) cosmic rays primarily responsible for ionizing the ISM are not observable at Earth due to the magnetic field coupled to the solar wind. Because they are easily deflected, we have no direct measure of the interstellar cosmic ray spectrum, and must instead attempt to compute the ionization rate from other observables. Some of these observables include molecules such as OH, HD, and H_3^+, all of which form due to an initial ionization of the ambient hydrogen. However, cosmic-ray ionization rates inferred from each of these tracers have differed by about 2 orders of magnitude for the same sight line. Results also vary between diffuse and dense clouds as the dense clouds have a higher stopping power and thus limit the entry of lower energy cosmic rays. The difference in this case is a cosmic-ray ionization rate about 1 order of magnitude higher in diffuse clouds than in dense clouds. Finally, there may be localized sources of cosmic rays in the ISM which can lead to spatial fluctuations in the ionization rate.

Together, all of these difficulties leave the cosmic-ray ionization rate in a somewhat uncertain state. It is my goal to use multiple tracers in various environments in an attempt to resolve this issue. Independent checks should serve to better constrain the ionization rate. In concert with theory, it is my hope that new observations will lower the uncertainty of the cosmic-ray ionization rate, and provide a value which can be used more confidently in astrochemical modeling.

2. COMPONENTS OF THE INTERSTELLAR MEDIUM

Adopting the classification scheme of Snow & McCall (2006), we further divide the Cold Neutral Medium (CNM) phase of the ISM into four cloud categories: diffuse atomic, diffuse molecular, translucent, and dense molecular. The quantitative way of distinguishing between cloud types involves the fraction of nuclei of a given species in a given form, for example, the fraction of hydrogen nuclei in molecular form. This fraction is expressed as

$$f_{H_2}^n = \frac{2n(H_2)}{n(H) + 2n(H_2)} \tag{1}$$

where the subscript refers to the species in question, and the superscript n means this is calculated from a localized number density. This fraction can also be calculated using the observed column densities, $f_{H_2}^N$, but in this case the fraction is almost certainly an underestimate of the localized fraction in denser regions because the integrated line-of-sight includes atomic material not associated with the cloud. Similarly, this fraction can be computed for carbon species when it is assumed that all carbon is in the form of C^+, C, or CO. Using these fractions, the 4 cloud types above are defined by the following properties: diffuse atomic – $f_{H_2}^n < 0.1$; diffuse molecular – $f_{H_2}^n > 0.1$, $f_{C+}^n > 0.5$; translucent – $f_{C+}^n < 0.5$, $f_{CO}^n < 0.9$; dense – $f_{CO}^n > 0.9$. Figure 1, a reproduction of Figure 1 from Snow & McCall (2006), schematically shows the transition of hydrogen and carbon species between each cloud type.

Due to the variation in composition between cloud types, there is a distinct difference in the chemistry that occurs in each environment. The following summaries are largely paraphrased from Snow & McCall (2006). Diffuse atomic clouds are exposed to stellar radiation and so molecules that form are quickly dissociated. My study is not concerned with the chemistry of these regions, so I will not discuss them further. Diffuse molecular clouds provide enough self shielding so that a significant fraction of the hydrogen is in molecular form. This allows for simple chemical processes to form species such as CO, CN, CH, C_2, H_3^+, OH, and HCO^+. However, there is enough radiation to keep most of the carbon in ionized form, C^+, thus providing a large number of free electrons. In translucent clouds the material is protected enough from radiation so that carbon begins the transition to neutral atomic form and carbon monoxide. Finally, the carbon in dense molecular clouds is primarily in the form of CO. Due to the lack of ionizing radiation and electrons, reactions are free to proceed in this environment without the products being quickly destroyed.

The progression of densities between cloud types leads to the prediction that the cosmic-ray ionization rate should differ in each environment. This stems from two separate processes. The first, cosmic-ray self-confinement, is discussed by Skilling & Strong (1976) and Padoan & Scalo (2005). In this process, the cosmic rays generate Alfvén waves which actually

confine lower energy particles ($\lesssim$100 MeV) to diffuse material. The second process involves the energy loss and effective range of cosmic rays. Lower energy particles ($\lesssim$20 MeV) are unable to penetrate far enough into dense clouds to have any effect on the internal chemistry (Cravens & Dalgarno 1978). If this progression can be observed in the ionization rates inferred from H_3^+, it will be a significant test of the calculations discussed in the following section.

3. BACKGROUND CHEMISTRY

Of the molecules mentioned above, H_3^+ has the simplest chemistry when considered in both diffuse and dense clouds. Its formation and destruction processes in diffuse clouds are given by the reactions:

$$CR + H_2 \rightarrow CR + H_2^+ + e^-, \tag{2}$$

$$H_2 + H_2^+ \rightarrow H_3^+ + H, \tag{3}$$

$$H_3^+ + e^- \rightarrow H_2 + H \text{ or } 3H. \tag{4}$$

H_2 is first ionized, resulting in an H_2^+ ion and an electron. We assume that this ionization is due only to cosmic rays because Glassgold & Langer (1974) showed that X-rays are attenuated in a thin layer at the exterior of diffuse clouds. The H_2^+ ion then reacts with H_2 to produce H_3^+ and H. The first reaction in the process is the rate limiting step as it is many orders of magnitude slower than the second (McCall et al. 1998). This means that the formation rate of H_3^+ is essentially the ionization rate of H_2. The primary channel for destroying H_3^+ in diffuse clouds is recombination with an electron, which results in either three hydrogen atoms, or one hydrogen atom and one molecule. The steady state approximation assumes that the formation and destruction rates of H_3^+ are equal, and yields the equation (Geballe et al. 1999)

$$n(H_2)\zeta_2 = k_e n(H_3^+)n(e), \tag{5}$$

where $n(X)$ is the number density of species X, ζ_2 is the ionization rate of H_2, and k_e is the H_3^+-electron recombination rate constant. Making some substitutions and assumptions, we can manipulate this to be

$$\zeta_2 = 2N(H_3^+)\frac{n_H}{f_{H_2}^N}\frac{k_e}{N_H}\left[\frac{n(e)}{n_H}\right], \tag{6}$$

where $N(X)$ is the column density of species X, n_H is the number density of hydrogen nuclei, and $f_{H_2}^N$ is the fraction of hydrogen nuclei in molecular form (see § 4.2 of Indriolo et al. (2007) for an in depth discussion of our assumptions). In this form it is possible to measure or estimate all of the variables on the right hand side of the equation, so we can derive values for the ionization rate of molecular hydrogen.

For dense clouds, however, the primary destruction mechanism of H_3^+ is different. In such regions, reaction (4) is replaced with the two reactions:

$$H_3^+ + CO \rightarrow HCO^+ + H_2, \tag{7}$$

$$H_3^+ + O \rightarrow OH^+ + H_2, \tag{8}$$

thus changing equation (5) to

$$n(H_2)\zeta_2 = n(H_3^+)[k_{CO}n(CO) + k_O n(O)]. \tag{9}$$

We can perform similar manipulations and assumptions here to produce the dense cloud analog of equation (6), thus allowing us to infer the cosmic-ray ionization rate in this environment as well.

The steady state analyses for OH and HD are significantly more complicated. The formation routes for these begin with the charge transfers from H^+ to either O or D, both of which are endothermic. These two processes compete with each other, as well as electron recombination and grain neutralization, to remove the available H^+. With the variety of possible branches, it is more difficult to use OH or HD abundances to back out the ionization rate of atomic hydrogen. Still, Federman et al. (1996) derived analytical expressions which can be used to find the ionization rate of atomic hydrogen, ζ_H, given the OH or HD columns and several other parameters.

Along with the molecules above, it is also possible to use atomic tracers in calculating the cosmic-ray ionization rate. Metastable helium, He^*, is one such tracer, and like H_3^+, its chemistry is relatively simple. Producing He^* is a two step process where neutral helium is first ionized by a cosmic ray to form He^+, which then recombines with an electron to reach the metastable state. During this recombination step though, there is a chance that the He will either end up in the singlet or triplet manifold, and only the triplet manifold leads to the metastable state. The first step is a few orders of magnitude slower than the second step, so the rate of formation of He^* can be approximated by the rate of the first step and the branching fraction of the second step. Metastable helium is destroyed by the doubly forbidden ($\Delta S \neq 0; \Delta L = 0$) spontaneous emission back to the ground state. Once again assuming steady state gives the expression:

$$\Gamma_3 n(He)\zeta_{He} = n(He^*)A, \tag{10}$$

where Γ_3 is the fraction of He^+ that recombines into the triplet manifold, $n(He)$ is the number density of helium in the ground state, ζ_{He} is the ionization rate of helium, $n(He^*)$ is the number density of helium in the metastable state, and A is the Einstein coefficient.

Assuming a uniform distribution of material, we can replace the number densities with column densities and rearrange the equation to be:

$$\zeta_{\text{He}} = \frac{A}{\Gamma_3} \frac{N(\text{He}^*)}{N(\text{He})}. \tag{11}$$

Using this process, we can determine the cosmic-ray ionization rate completely independently of H_3^+.

4.   OBSERVATIONS

At present, observations have been made searching for all of the above tracers in attempts to determine the cosmic-ray ionization rate in diffuse clouds. We have experience with H_3^+ and He*, but have not repeated any of the OH and HD observations performed over the past few decades.

4.1.   Methods

All of our H_3^+ and He* observations were made using the CGS4 spectrometer (Mountain et al. 1990) on the United Kingdom Infrared Telescope (UKIRT) at Mauna Kea. Settings were selected to provide a high resolving power of about 40000, necessary for detecting the weak H_3^+ lines. The slit was nodded in a standard ABBA pattern for the purpose of removing the atmospheric background. Suitable standard stars were observed throughout each night to account for changing atmospheric conditions and air mass. To aid in the confirmation of an H_3^+ detection, we observed both the $R(1,1)^u$ and $R(1,0)$ transitions at 3.66808 μm and 3.66852 μm, respectively. For He*, we attempted to observe the He I line at 1.08333 μm. Once the spectra were taken, we used standard astronomical software packages to reduce the data. Some examples showing detections of H_3^+ from which our calculations are done are shown in Figure 2.

4.2.   Results

The ionization rate of atomic hydrogen, ζ_H, was calculated by several groups (Black & Dalgarno 1977; Black et al. 1978; Hartquist et al. 1978; Federman et al. 1996) using measurements of the column density of OH along various sightlines. Typical results were on the order of a few times 10^{-17} s^{-1}. Using HD columns, O'Donnell & Watson (1974) obtained

similar results. Because the observational results of the time were consistent with each other, a "canonical" ionization rate of about 3×10^{-17} s^{-1} was adopted in the literature for several years for both diffuse and dense clouds.

H_3^+ was first used as a means of inferring the cosmic-ray ionization rate by McCall et al. (2003) where they calculated $\zeta_2 = 1.2 \times 10^{-15}$ s^{-1}. Surprisingly, this value is over an order of magnitude larger than the widely adopted canonical rate. In further support of this high ionization rate, we surveyed 19 diffuse clouds for H_3^+ and found an average rate for ζ_2 of about 5×10^{-16} s^{-1} (Indriolo et al. 2007). The ionization rates along different sightlines covered a range of values a few times larger and smaller than this average, but as our calculations include uncertainties of about a factor of 3 either way, nothing conclusive can be said about the variations.

While metastable helium would provide an important independent check on the ionization rate, we have yet to successfully detect it in the ISM. So far, two attempts have been made. The first observation, toward HD 229059, was hampered by a strong emission feature in the background star. The observation toward HD 183143, shown in Figure 3, does not have a high enough signal-to-noise ratio (S/N) to detect the extremely weak line. After discussions with Lew Hobbs, our collaborator, we determined that a S/N$\sim$1000 may be necessary to achieve a 3σ detection. Presently, we have an observing program in queue on the Gemini South Telescope which should provide the necessary results when the data are taken early this summer.

5. THEORY

In addition to the observational methods for inferring the cosmic-ray ionization rate, there are also various theoretical approaches. The two most prevalent means are the extrapolation of the low energy cosmic ray spectrum from high energy observations, and the prediction of abundances via cloud models and simulations using different input parameters.

5.1. Cosmic Ray Spectrum

The first attempts at determining the ionization rate by extrapolating the observed cosmic ray spectrum were made by Hayakawa et al. (1961) and Spitzer & Tomasko (1968) who computed values of $\zeta_H = 10^{-15}$ s^{-1} and $\zeta_H > 6.8 \times 10^{-18}$ s^{-1}, respectively. Since those initial studies, the calculation has been performed several times with a different cosmic ray spectrum in each case. The most recent calculation was performed by Webber (1998), who

computed an ionization rate of $(3-4) \times 10^{-17}$ s^{-1} using a cosmic ray spectrum extrapolated from data taken with the *Pioneer* and *Voyager* spacecraft. This took advantage of the fact that at the positions of the spacecraft, beyond 40 AU away from the sun, cosmic rays are less affected by the weaker solar magnetic field.

In addition to producing the observables discussed so far, cosmic rays have a further impact on the ISM. Most notably, cosmic-ray spallation of C, N, and O nuclei is responsible for producing a great deal of ^{6}Li, ^{7}Li, ^{9}Be, ^{10}B, and ^{11}B, often collectively referred to as LiBeB. Cosmic rays can also excite nuclear states of C and O which emit 4.4 MeV and 6.13 MeV gamma rays, respectively, upon de-excitation. This means that on top of predicting the observed ionization rate of hydrogen, any cosmic ray spectrum chosen should also reproduce the observed light element abundances and gamma ray line fluxes.

Taking these constraints into account, we have begun an attempt to find a cosmic ray spectrum that can reproduce all of the expected observables. Our preliminary results suggest that in obtaining an ionization rate of 10^{-16} s^{-1}, light elements are produced in abundances roughly in accord with those measured in meteorites and interstellar gas. As for the gamma rays, we predict a diffuse Galactic flux that is slightly below observable limits using current telescopes, so this test is inconclusive at present. I plan to continue along this line of work in an attempt to better constrain the low energy cosmic ray spectrum.

5.2. Astrochemical Models and Simulations

The modeling of chemical reactions in astrophysical conditions has also been performed extensively over the past several decades. Many of these models use conditions specific to a particular sight line as input parameters to then predict the abundances of several atomic and molecular species. Studies by Black & Dalgarno (1977), Black et al. (1978), and van Dishoeck & Black (1986) represent some of the earlier works along these lines. For the most part, these models were able to predict abundances within a few times the observed values. However, in some cases certain chemical and physical effects were not taken into account, and some reaction rate constants were not the same as more recently measured values. The result of such unintentional omissions is that several predicted abundances may not have been correct.

Studies in the past few years have tried to account for some of these other effects. Liszt (2003) emphasized the importance of grain neutralization originally proposed by Lepp et al. (1988). This process reduces the number of H$^+$ ions in the gas through charge transfer with small grains. By lowering the abundance of H$^+$, the production rates of both HD and OH

will decrease due to their dependencies on the initial charge transfer reaction mentioned previously. With grain neutralization included, the model of Liszt (2003) requires an ionization rate of $\zeta_H \geq 2 \times 10^{-16}$ s^{-1} to reproduce both the observed HD and H$_3^+$ column densities. Le Petit et al. (2004), however, invoked a three-phase model which included diffuse gas, dense gas, and magnetohydrodynamic shocks along the specific sight line toward ζ Per. They found that the ionization rate which best reproduced the most observed abundances was $\zeta_H = 2.5 \times 10^{-16}$ s^{-1}. Together, these newer simulations seem to be consistent with the results inferred from our H$_3^+$ observations.

6. FUTURE WORK

6.1. Overview

My goal over the next few years is to address the problem of constraining the cosmic-ray ionization rate in various environments by using several observational tracers and theoretical predictions. As a continuation of my previous work, this will include further observations of H$_3^+$ in the ISM. While we believe H$_3^+$ to be the most reliable tracer because of its simple chemistry, it is still a useful check to use as many observables as possible. This means searching for OH, HD, and He* wherever the observations are feasible. On the theory side, our calculations should be refined to include further effects such as cosmic ray propagation and the destruction of the light elements in stellar interiors. This will produce more realistic results which can be compared to observational abundances. Together, these projects should allow us to better constrain both the cosmic-ray ionization rate in the ISM and the cosmic ray spectrum at low energies.

6.2. Observing Plans

Gathering the data necessary for this project will require several observations. To simplify the proposal process, it seems natural to divide the observations into groups based on cloud type and molecular (or atomic) tracer.

We currently have H$_3^+$ data toward about 20 diffuse cloud sight lines, but only a handful of these have been surveyed for OH and HD (see Table 1 for a list of these and some of the relevant data). As such, it would be helpful to obtain OH and/or HD data for more of these sight lines to act as independent checks. Unfortunately, with no space based telescopes currently operating in the 1000 Å range, the only opportunity to find more HD observations is by mining *Copernicus* and *FUSE* data. OH, on the other hand, is observable from ground

based telescopes using absorption lines at 3078 Å and 3081 Å. These lines were studied by Federman et al. (1996) toward a few sight lines, so I know that the observations are feasible, if a bit time consuming. As previously discussed, metastable helium involves relatively simple chemistry, but is extremely difficult to detect. However, the conditions are favorable in a few sight lines beyond HD 183143, and I plan to submit more proposals to search for the He I line at 1.08333 μm.

Dense clouds have also been surveyed for H_3^+, but not to the extent of diffuse clouds. Combined, Geballe & Oka (1996) and McCall et al. (1999) searched about 15 clouds for H_3^+. Properties of these are also given in Table 1. For these sight lines I have yet to perform the calculation of the ionization rate using the methods listed in § 3. This will be done in the near future once all of the necessary variables have been determined or approximated, thus providing ζ_2 in dense clouds. Due to the large extinction associated with dense clouds though, the UV spectra of OH and HD cannot be measured, eliminating two of my independent checks. On the other hand, the large reservoir of CO leads to the production of HCO^+ which has also been used as an indicator of the ionization rate via modeling (van der Tak & van Dishoeck 2000). To better constrain the cosmic-ray ionization rate in dense clouds then, I plan to search for H_3^+ in sight lines that also have HCO^+ measurements so that I have another check.

Unlike diffuse and dense clouds, translucent clouds have not been well studied. Part of this is due to the difficulty in conclusively proving that a given sight line is translucent. For example, a large extinction may be caused by several diffuse clouds "piled up" along the sight line. Using the quantitative definitions from § 2, we need CO measurements to better classify translucent clouds. We currently have CO observations toward a few sight lines believed to be translucent, but the analyses have yet to be performed. Furthermore, we have 6 hours of time on the Infrared Telescope Facility (IRTF) this May to measure CO toward 3 such targets. In addition to CO, we have observed H_3^+ in a few sight lines thought to pass through translucent clouds. However, the present sample of translucent sight lines with both H_3^+ and CO observations totals only 3. To increase the sample, I am planning H_3^+ and CO observations toward several translucent clouds which are also targets of a COS (Cosmic Origins Spectrograph) survey led by our collaborator, Ted Snow. Using guaranteed time on *Hubble*, he plans to observe C and C^+ in these sight lines, which will provide us with data useful in determining the ionization rate in this environment. When completed, I should have the necessary observations through about 10 translucent clouds.

In all cases, H_3^+ will be observed using the aforementioned $R(1,1)^u$ and $R(1,0)$ transitions at 3.66808 μm and 3.66852 μm, respectively. These arise from the lowest two rotational levels, the only levels populated at the low temperatures of the ISM in the environments we study.

As a result, they essentially probe the complete H_3^+ population. To detect CO, we use the R(3), R(2), R(1), R(0), P(1), and P(2) transitions of the $\nu = 1 - 0$ vibrational band located near 4.65 μm. Because of atmospheric CO though, observations must be planned so that the Doppler shift resulting from the Earth's motion moves the interstellar lines away from their rest wavelengths.

6.3. Theoretical Calculations

From all of the above planned observations, we will gain further constraints on the low energy cosmic ray spectrum. As mentioned before, the different densities of each cloud type result in different depths to which low energy cosmic rays can penetrate. This property predicts a gradual decrease in the ionization rate from diffuse to dense clouds. After calculating the ionization rate in diffuse, translucent, and dense clouds from observations, we can search for a low energy cosmic ray spectrum that reproduces the results.

In addition to reproducing the various ionization rates, this spectrum will still need to successfully predict light element abundances and gamma ray fluxes. To continue along these lines, the physics included should be advanced beyond our current model. Most importantly, propagation effects and the depletion of light elements should be taken into account. Our current model assumes a constant cosmic ray spectrum in space and time, and that all light elements produced remain in the ambient gas. While these assumptions should produce rough results for the time being, the inclusion of more physical effects will improve our results and make them more readily comparable to observables.
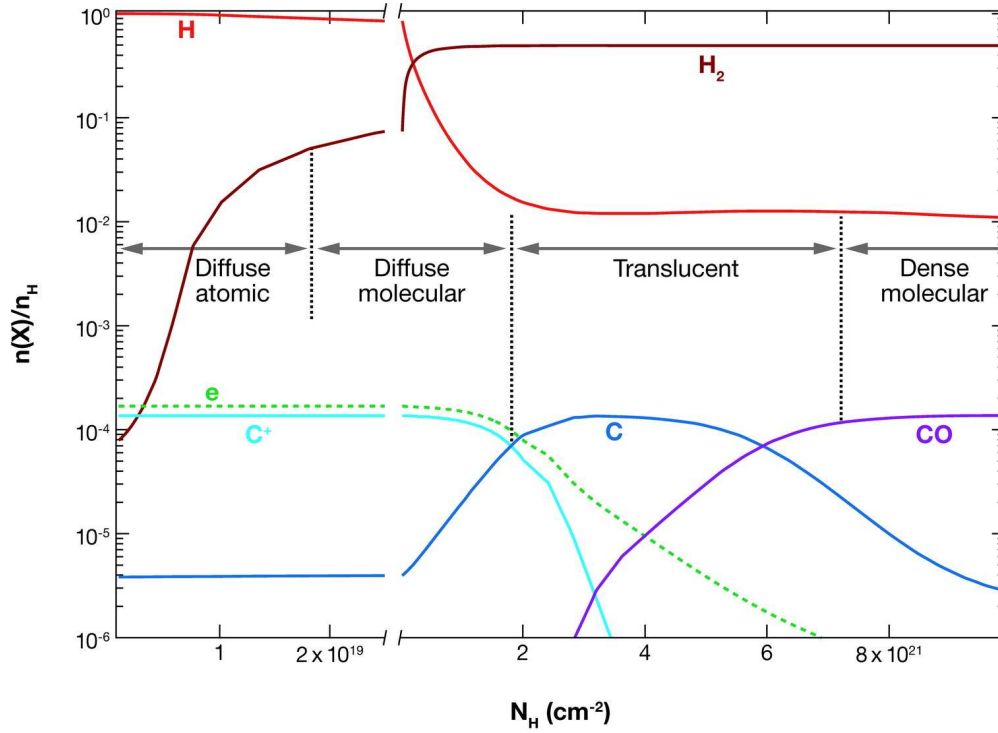
6.4. Relevance

When completed, the proposed observations and theory work should provide three important results. First, we should have much better constraints on the cosmic-ray ionization rate. The combined use of H_3^+, OH, HD, and He^* means that we will have several independent estimates of the ionization rate. A more accurate ionization rate in multiple environments means that cloud models will do better jobs of reproducing observable molecular abunances. Second, the survey of CO and H_3^+ in translucent clouds will produce data for this little-studied environment of the ISM. These data will help to determine both the ionization rate and molecular fraction, and will be combined with the results from the COS survery along with several other ancillary observations which are either planned or underway, and cover wavelengths ranging from the millimeter to ultraviolet. Finally, the transition from diffuse to

dense clouds will allow the constraint of the low energy cosmic ray spectrum through theory and particle astrophysics. As there is no way to directly constrain this unobservable part of the spectrum, this work should prove extremely useful to the understanding of cosmic ray acceleration mechanisms. Overall, these results should culminate in a better understanding of some fundamental properties of the ISM.

REFERENCES

Black, J. H., & Dalgarno, A. 1977, ApJS, 34, 405

Black, J. H., Hartquist, T. W., & Dalgarno, A. 1978, ApJ, 224, 448

Cravens, T. E., & Dalgarno, A. 1978, ApJ, 219, 750

Federman, S. R., Weber, J., & Lambert, D. L. 1996, ApJ, 463, 181

Geballe, T. R., & Oka, T. 1996, Nature, 384, 334

Geballe, T. R., McCall, B. J., Hinkle, K. H., & Oka, T. 1999, ApJ, 510, 251

Glassgold, A. E., & Langer, W. D. 1974, ApJ, 193, 73

Hartquist, T. W., Black, J. H., & Dalgarno, A. 1978, MNRAS, 185, 643

Hayakawa, S., Nishimura, S., & Takayanagi, T. 1961, PASJ, 13, 184

Indriolo, N., Geballe, T. R., Oka, T., & McCall, B. J. 2007, ApJ, 671, 1736

Le Petit, F., Roueff, E., & Herbst, E. 2004, A&A, 417, 993

Lepp, S., Dalgarno, A., van Dishoeck, E. F., & Black, J. H. 1988, ApJ, 329, 418

Liszt, H. 2003, A&A, 398, 621

McCall, B. J., Geballe, T. R., Hinkle, K. H., & Oka, T. 1999, ApJ, 522, 338

McCall, B. J., Geballe, T. R., Hinkle, K. H., & Oka, T. 1998, Science, 279, 1910

McCall, B. J., et al. 2002, ApJ, 567, 391

McCall, B. J., et al. 2003, Nature, 422, 500

Mountain, C. M., Robertson, D. J., Lee, T. J., & Wade, R. 1990, Proc. SPIE, 1235, 25

O'Donnell, E. J., & Watson, W. D. 1974, ApJ, 191, 89

Padoan, P., & Scalo, J. 2005, ApJ, 624, L97

Skilling, J., & Strong, A. W. 1976, A&A, 53, 253

Snow, T. P., & McCall, B. J. 2006, ARA&A, 44, 367

Spitzer, L., Jr., & Tomasko, M. G. 1968, ApJ, 152, 971

van der Tak, E. F. S., & van Dishoeck, E. F. 2000, A&AL, 358, L79

van Dishoeck, E. F., & Black, J. H. 1986, ApJS, 62, 109

Webber, W. R. 1998, ApJ, 506, 329

– 13 –

Fig. 1.— Reproduction of Figure 1 from Snow & McCall (2006) showing the hydrogen and carbon fractions as a function of cloud column density.
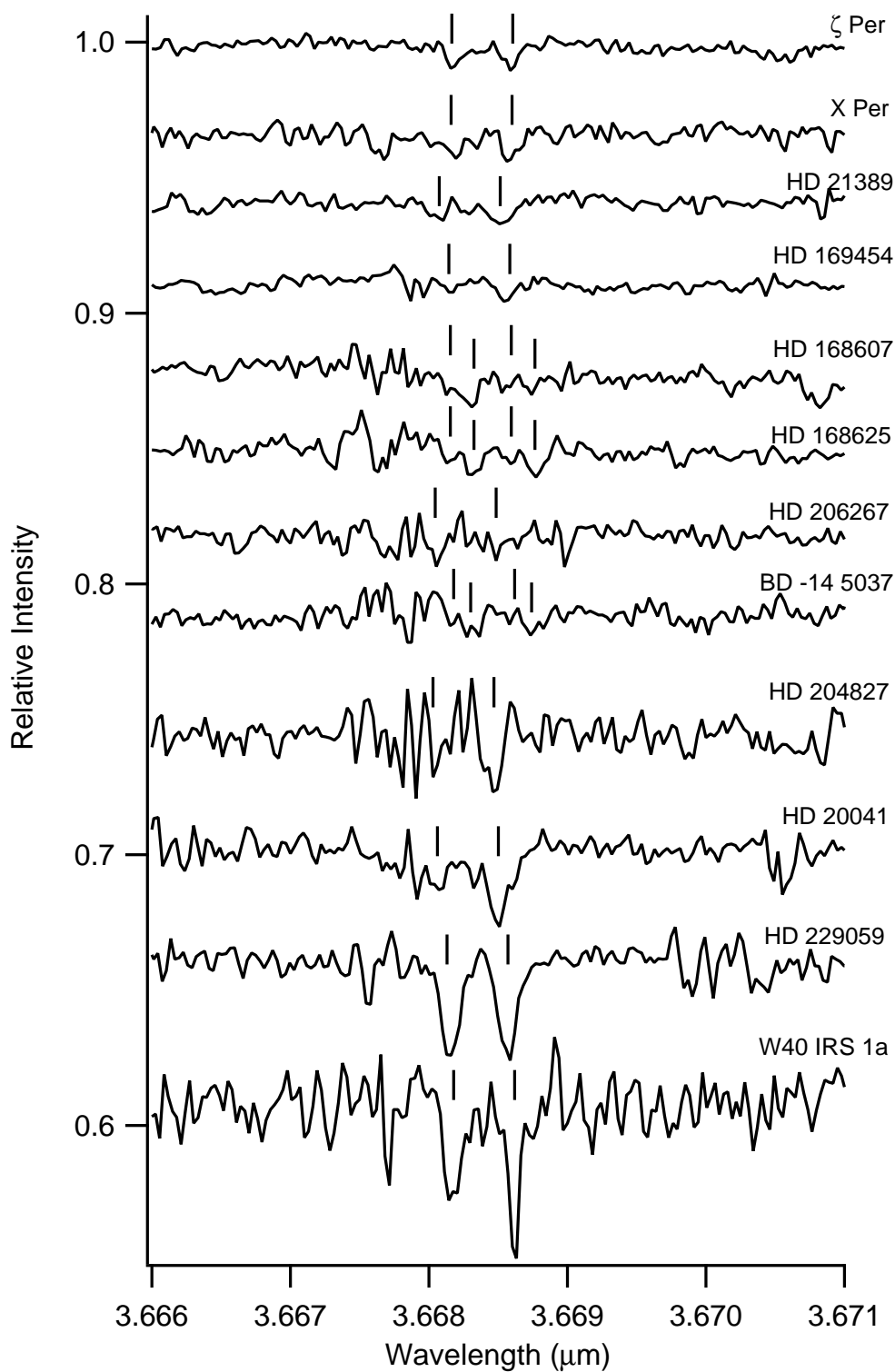
Fig. 2.— Spectra showing detections of H_3^+ in diffuse clouds. Lines indicate the predicted location of the H_3^+ absorption from previous velocity measurements. Vertical offsets are made for the sake of clarity. All spectra have been shifted in wavelength to be at rest in the local standard of rest frame.
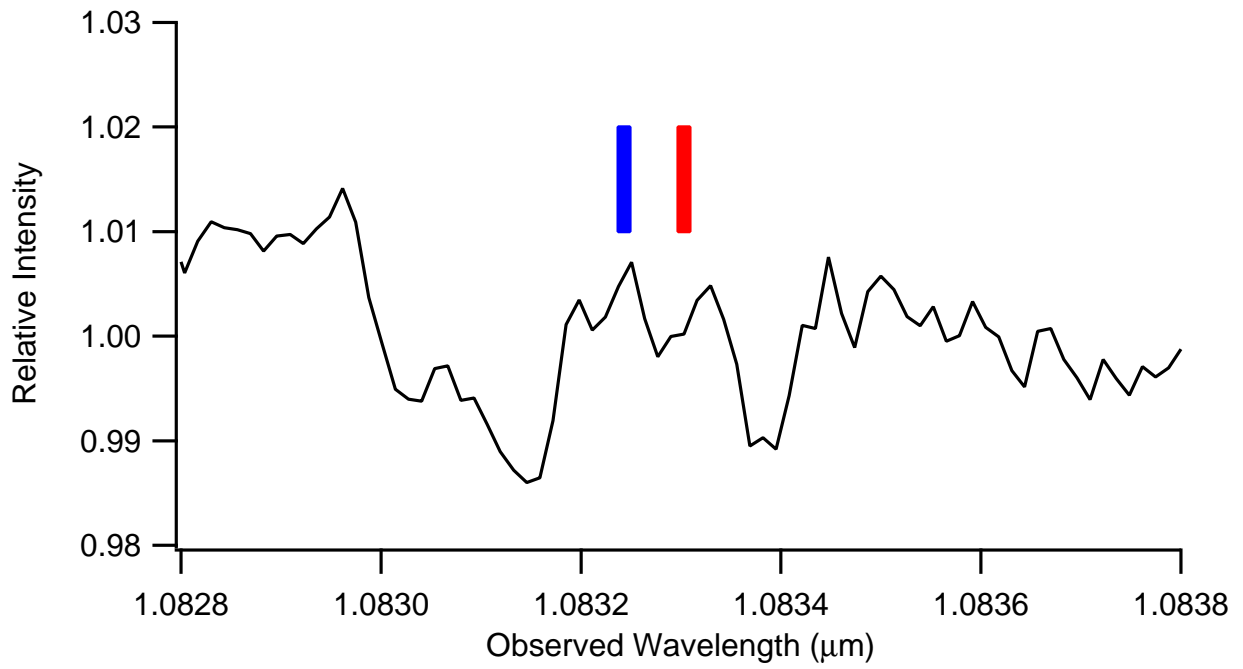
Fig. 3.— Spectrum showing the predicted location of the metastable helium line. The two bars indicate the range of previous measurements of two velocity components along the sight line towards HD 183143.

Table 1.   Some Parameters for Observed Sightlines

Object	Cloud Type	ζ_2 $(10^{-16}\ \mathrm{s}^{-1})$	$N(\mathrm{H_3^+})$ $(10^{14}\ \mathrm{cm}^{-2})$	relevant observations
HD 20041	diffuse	6.7	1.6	...
HD 21389	diffuse	4.1	0.8	...
ζ Per	diffuse	7.3	0.7	OH, HD
X Per	diffuse	7.1	0.8	...
HD 206267	diffuse	3.3	0.6	...
W40 IRS 1a	diffuse	3.5	3.3	...
WR 104	diffuse	3.2	2.3	CO
WR 118	diffuse	4.7	6.5	CO
WR 121	diffuse	3.9	2.2	...
Cyg OB2 5	diffuse	3.5	2.6	CO
Cyg OB2 12	diffuse	4.0	3.8	CO
HD 183143	diffuse	5.3	2.3	CO, He*
HD 21483	diffuse	<13	<2.2	...
40 Per	diffuse	<5.9	<0.9	...
o Per	diffuse	<11	<0.6	OH, HD
ϵ Per	diffuse	<5.5	<0.5	HD
ξ Per	diffuse	<10	<0.5	OH, HD
62 Tau	diffuse	<33	<2.7	...
o Sco	diffuse	<1.1	<0.3	...
ζ Oph	diffuse	<1.6	<0.1	OH, HD
λ Cep	diffuse	<3.0	<0.9	...
χ^2 Ori	diffuse	<4.7	<0.7	...
P Cyg	diffuse	<2.8	<0.6	...
HD 169454	translucent	1.2	0.3	...
HD 168607	translucent	1.3	0.7	...
HD 168625	translucent	3.1	1.0	CO
HD 204827	translucent	6.3	1.1	...
HD 229059	translucent	6.8	3.4	He*
HD 147888	translucent	<6.3	<1.2	...
HD 147889	translucent	<2.6	<0.4	...

Table 1—Continued

Object	Cloud Type	ζ_2 $(10^{-16}\ \mathrm{s}^{-1})$	$N(\mathrm{H}_3^+)$ $(10^{14}\ \mathrm{cm}^{-2})$	relevant observations
HD 29647	translucent	...	NR	CO
NGC 2024 IRS 1	translucent	...	NR	CO
BD -14 5037	??	1.6	0.6	...
HD 194279	??	<2.9	<1.2	...
AFGL 2136	dense	...	3.8	CO, HCO$^+$
W 33A	dense	...	5.2	CO, HCO$^+$
Mon R2 IRS 3	dense	...	1.4	CO
AFGL 961E	dense	...	1.7	CO
AFGL 490	dense	...	1.1	CO, HCO$^+$
AFGL 2591	dense	...	2.2	CO, HCO$^+$
Orion BN	dense	...	<1.8	...
NGC 2024 IRS 2	dense	...	<1.0	...
Mon R2 IRS 2	dense	...	<1.5	...
AFGL 989	dense	...	<0.8	...
Elias 29	dense	...	<1.8	...
M17 IRS 1	dense	...	<7.8	...
W3 IRS 5	dense	...	<0.8	CO, HCO$^+$
S140 IRS 1	dense	...	<0.4	CO, HCO$^+$
LkHα 101	dense	...	<1.0	...

Note. — The above columns include the target star, cloud type, ionization rate of H$_2$, ζ_2, total H$_3^+$ column density, $N(\mathrm{H}_3^+)$, and a list of the other important tracers observed. Most values are compiled from or based on data from McCall et al. (1999), McCall et al. (2002), and Indriolo et al. (2007), with a few coming from more recently acquired but unpublished data. An entry of NR means that the data have been taken but not yet reduced.